X-616-68-335

PREPRINT

NASA TM X- 63327

Recent Results from Lunar Explorer 35*

Norman F. Ness

Laboratory for Space Sciences
NASA-Goddard Space Flight Center
Greenbelt, Maryland USA 20771

September 1968

*Presented at Conference on the Physics of the Moon and Planets
Kiev, USSR October, 1968

Extraterrestrial Physics Branch Preprint Series

Abstract

Recent measurements since July 1967 from lunar orbit by Explorer 35 have provided significant data on the moon and its environment. When the moon is imbedded in the geomagnetic tail, no intrinsic lunar magnetic field is detected, limiting its magnetic moment to 10^{20} cgs units, less than 10^{-6} of the earth's. This corresponds to an intrinsic lunar field of less than 40 μ Gauss on the lunar surface. The magnetic susceptibility of the moon is less than 1.8 μ_o if the interior is below the Curie point. In interplanetary space no evidence is found for a bow shock wave due to the flow of the supersonic solar wind plasma past the moon. A solar plasma shadow or cavity evolves on the nightside of the moon as the moon absorbs the plasma with small perturbations of the magnitude and direction of the interplanetary magnetic field. The imbedded interplanetary magnetic field appears to diffuse as rapidly through the interior of the moon as the solar wind convectively transports it past the moon. This precludes accretion of the magnetic field as theorized by Gold and Tozer and is due to the low effective electrical conductivity of the moon, less than 10^{-5} mhos/meter. This value suggests relatively low temperatures of the interior of approximately 1000°K. This assumes a temperature dependency of electrical conduction of lunar material similar to terrestrial magnesium-iron silicates. The moon appears to be a nonmagnetic, relatively non-conducting, dielectric, cold sphere.

1.0 Introduction

During 1963-1965 the small spin stabilized satellites Explorers 18, 21 and 28 represented the initial phase of the USA IMP (Interplanetary Monitoring Platform) program to study the geophysical environment of the earth from highly eccentric orbit. Principal results were definitive measurements of the solar wind interaction with the geomagnetic field and a study of the interplanetary magnetic field.

The solar wind is the supersonic expansion of the solar corona plasma into interplanetary space. It is composed primarily of protons and electrons with a small (less than 10%) admixture of doubly ionized helium and smaller amounts of heavier elements in various states of ionization. At the orbit of earth the solar wind velocity varies between 300 to 800 km/sec with a typical density of 5 protons/ cm^3. This represents a proton energy of from 400 eV to 4 keV and a flux of approximately 3×10^8 protons/cm^2/sec. Imbedded in this plasma is an extended solar magnetic field of 3 to 8γ ($1\gamma=10^{-5}$ oersted).

The electron and ion temperatures are not equal and the thermal motion of the ions anisotropic[6]. The temperature of the ions is approximately 10^5 ^oK with $T_{\parallel}/T_{\perp}$ varying between 1.5 and 4. The electron temperatures are found to be 1-3 times the ion temperatures. The length scales of interest in the solar wind vary from a collision length of the order of 1 AU to the ion gyroradius of the order of 50 km and the Debye length of the order of 10 meters. Both the Alfvén and ion thermal velocities in cislunar space are approximately 50 km/sec so that the Mach number of solar wind flow is approximately 10.

Because of the different magnetic properties of the moon and the earth, the interaction of the solar wind with these two bodies is vastly different. The main features of the earth's case are: (i) the formation of a magnetosphere around which the bulk of the solar plasma flows, (ii) the development of an extended magnetic tail in the antisolar direction, and (iii) the presence of a detached, collisionless bow shock wave upstream from the magnetosphere.

Early results in 1959 from Luna 2 indicated the absence of a strong lunar magnetic field, setting an upper limit of 100γ for the magnitude on the lunar surface. Gold[5] and subsequently Tozer and Wilson[16] postulated that in the absence of a sufficiently intense lunar field the solar wind would directly impact the lunar surface and the imbedded interplanetary magnetic field would be captured due to the high electrical conductivity of the lunar interior. A pseudo-magnetosphere and attached shock wave would be formed as shown for this model in Figure 1. Measurements by Luna 10 in 1966 were interpreted as indicating the existence of a pseudo-magnetosphere although no evidence for a shock wave was reported[3].

This paper summarizes the results from Explorer 35 which show the absence of both a pseudo-magnetosphere and a shock wave. In addition these measurements have been used to study the magnetic susceptibility, electrical conductivity and internal temperature of the moon.

2.0 Satellite and Orbit

The initial attempt to study the environment of the moon by anchoring an IMP type satellite in lunar orbit in 1966 failed with Explorer 33 placed instead into an extremely high apogee-perigee earth orbit from which significant scientific results have been obtained. The second attempt on 19 July 1967 was successful with Explorer 35 placed into lunar orbit on July 22 with orbital period 11.53 hours, inclination 169° with respect to the ecliptic plane, aposelene = 9388 ± 100 km ($5.4\ R_M$, R_M = Radius of Moon = 1738 km) periselene = 2568 ± 100 km ($1.4\ R_M$) and initial aposelene-moon-sun angle = 304° East.

Figure 2 presents the projection of the orbit on a plane passing through the center of the moon and parallel to the ecliptic plane, which defines a selenocentric solar ecliptic coordinate system with the X_{SSE} axis directed from the moon to the sun and the Z_{SSE} axis perpendicular to the ecliptic plane. The variation of the orbit geometry is due to the heliocentric motion of the earth-moon system and leads to an apparent westward progression of the line of apsides of approximately 1.1° per day.

Explorer 35 is spin stabilized at 25.6 ± 0.4 RPM with the spin axis perpendicular to the ecliptic plane $\pm 2^{\circ}$. The spacecraft is powered by solar cells on four paddles although during passage through the optical shadow of the moon for intervals up to 60 minutes, battery power is required to continuously transmit scientific data.

The experiment repertoire includes two fluxgate magnetometers, two plasma probes, two energetic particle detectors and one cosmic dust detector. Two passive experiments utilize the spacecraft for a study of the gravitational field of the moon by analysis of its orbital characteristics and bistatic radar measurements of the electromagnetic properties of the lunar surface by monitoring the directly transmitted and lunar surface reflected RF signal.

The spacecraft has operated continuously since launch and successfully survived the long shadow periods during the lunar eclipses of 18 October 1967 and 13 April 1968. It has completed more than 900 orbits of the moon and as noted in Fig. 2 has provided direct measurements insitu of the lunar environment above 700 km.

3.0 Observations of Near Lunar Magnetic Field

As they orbit the earth, the moon and Explorer 35 are immersed repetitively in interplanetary space, the geomagnetosheath and the geomagnetotail. Data taken while the spacecraft is in the geomagnetic tail have been used to study the magnetostatic properties of the moon and while in interplanetary space to study its electrical conductivity.

When the moon is imbedded in the geomagnetic tail it is optimumly possible to detect any intrinsic magnetic properties of the lunar body. Data obtained from a detailed study[1] are shown in Fig. 3 for a "quiet" time as the spacecraft passes through periselene. The theoretical curve shown corresponds to superposition of a geomagnetic tail field of 9γ and a lunar magnetic moment of 10^{20} cgs units. Inspection indicates the observed perturbations are less than would be predicted with these parameters. This result is a factor of 60 lower than established by the Luna 2 results and the preliminary Explorer 35 results[11]. This suggests that the intrinsic magnetic field of the moon is less than 4γ on the surface and that in general the lunar magnetic field environment on the surface is dominated either by the geomagnetic tail, magnetosheath or interplanetary magnetic field depending upon the position of the moon relative to the geomagnetosphere. In addition, these data can be analyzed for magnetic susceptibility and the result obtained is that μ_M is less than $1.8\mu_o$ if the lunar body is homogeneous and its temperature below the Curie point[1].

Of special interest in this study are the periods when the moon is outside the earth's bow shock in the solar wind. During such times measurements of the magnetic field in the vicinity of the moon have been made during hundreds of spacecraft orbits. The characteristics of a bow shock (viz. a jump in field magnitude by a factor of 2-4 and substantial increase in fluctuations accompanying the heating of the plasma) have not been observed. The interplanetary magnetic field is observed to be only slighly perturbed by the presence of the moon[2, 11, 12, 15]. In the core of the lunar wake observations characteristically show an increase of the magnetic field $\lesssim$ 30% of the unperturbed value. In the penumbral regions, around this core, both positive and negative perturbations of the interplanetary field strength are often observed. The magnitude and geometry of the perturbations vary with conditions in the undisturbed solar wind, verified by simultaneous measurements with other satellites in cislunar space.

The major effect of the moon on the interplanetary medium is the creation of a plasma cavity[9, 13, 14]; the electrons and ions impacting the surface are absorbed by the lunar body. There is also no evidence for the development of a boundary layer analogous to the earth's magnetosheath. A small increase in the plasma flux in the penumbral region has been interpreted[14] as giving evidence of deflection of a small amount of plasma from the limbs of the moon.

A sample of magnetic field measurements in the lunar wake displaying relatively large perturbations of the magnetic field is shown in Figure 4. The spacecraft trajectory is shown projected on the ecliptic plane in the upper left hand corner and positionally correlated with the data through UT annotation. As the spacecraft enters the lunar wake region, an oscillating pattern of + - anomalies is detected. Subsequently after egression from the core region where a positive anomaly some 30% above the undisturbed field magnitude of approximately 5.7γ was detected, only a negative anomaly is again observed. Note that the latitude angle, θ, and longitude angle, ϕ, in selenocentric solar ecliptic coordinates, indicate the absence of appreciable directional variations of the fields through the lunar wake region.

Such large variations of the magnetic field in the lunar wake are not always observed. Frequently it is necessary to use simultaneous correlative data from another spacecraft in cislunar space to positively identify the umbral increase. With these results, it is clear that the theory shown in Fig. 1 is not valid and that there is no pseudo-magnetosphere formed since the interplanetary magnetic field is not accreted by the moon.

As noted by Johnson and Midgely[7], effects of a surface layer of low electrical conductivity may drastically alter the steady state conditions of solar wind flow past the moon. In order to study the internal electrical conductivity of the moon, it is necessary to investigate its dynamic response to discontinuities or sudden changes in the solar wind. The decay of eddy currents associated with such transients can then indicate the characteristic diffusion time of the lunar interior and thence its electrical conductivity.

Several large and very abrupt changes in the interplanetary magnetic field occurred in September 1967 when Explorer 35 was in the lunar wake close to the moon and Explorers 33 and 34 were simultaneously monitoring the interplanetary medium in cislunar space. A sample result is shown in Fig. 5 where it is seen that sudden changes occur in the lunar wake with time scales less than 5 seconds, and with a time signature nearly identical to that observed in the interplanetary medium unaffected by the moon.

An estimate of the electrical conductivity is possible if it is assumed that the time for convection of the solar wind discontinuity past the moon, τ_c, establishes an upper limit for the length of perturbations of the field due to eddy current decay. As shown in Fig. 6, τ_c ranges from 6-10 seconds so that depending upon the size of the conducting interior, the conductivity ranges from 10^{-6} to 10^{-5} $(\Omega\text{-m})^{-1}$. The data in Fig. 5 imply that $\tau_D \lesssim 5$ seconds.

England et al.[4] have studied various models of the electrical conductivity structure of the moon, a summary is shown in Fig. 7. Their work shows that if $\sigma_M < 10^{-5}$ $(\Omega\text{-m})^{-1}$ then the interior of the moon is relatively cool, less than 1000°C. In the case of concentrations of radioactive heat sources similar to chondritic meteorites, only a young moon has this property. If non-chondritic than the moon could be much older. In any event, the apparently low conductivity deduced from these observations strongly suggests a relatively cool lunar interior.

4.0 Electromagnetic Properties of Lunar Surface

Monitoring of the telemetry transmitter of Explorer 35 at 136 mHZ has been conducted by Stanford University using the transmitter as a radar beacon to remotely probe the electromagnetic properties of the moon's surface [17]. Radio signals which originate on the spacecraft are reflected from the lunar surface and both directly transmitted and lunar surface reflected signals are received at the Stanford antenna facilities.

As the spacecraft revolves around the moon the reflection point moves across the lunar surface at varying angles of incidence. Because the moon appears to be relatively smooth at the wave lengths employed, the reflection characteristics are principally dependent upon a small area only a few kilometers in extent. As the spacecraft passes behind and is occulted by the moon, a diffraction pattern is observed in the received signal.

The variation of the reflectivity versus angle of incidence is shown for both right and left hand circular polarizations in the upper portion of Fig. 8. The data were obtained on two days exactly one lunation apart with the variation in the response correlating with movement of the reflection point from highlands to the maria and back. A greater reflectivity is found in the maria and the general trend upward in reflectivity corresponds to motion of the reflection point onto relatively younger maria material in the region of Flamsteed. It is concluded that on the whole, the moon is a remarkedly homogeneous body with respect to reflection of electromagnetic signals at 136 mHZ. Typical variations are on the order of 30% although larger changes are occasionally observed. These variations are one order of magnitude less than what would be observed on the surface of the earth.

In the lower half of Fig. 8 are presented results pertinent to measurement of the Brewster angle of the lunar surface. This curve is the sum of the two circularly polarized scattered waves. The Brewster angle corresponds to that angle at which there is total absorption of linearly polarized waves and is found to be approximately 60^{o}. This implies a dielectric constant ϵ for the lunar surface of $3.0\epsilon_{o}$ at these wavelengths, 2.2 meters.

5.0 Kinetic Theory and Model of Solar Wind Flow Past Moon

A steady-state model for the plasma and field in the vicinity of the moon is considered here. Because the Larmor radius of charged particles is small (< 3%) compared with the dimension of the moon, each particle may be approximated by a guiding-center particle[19]. The lowest-order guiding-center gas has thermal motion only along the field lines, and thus under this approximation, the problem is reduced to the interaction between a sphere and a supersonic one-dimensional guiding-center gas.

In the interaction region, the guiding-center trajectory of ions is deflected slightly from a straight line by variations of the magnetic and the electric fields. Simple analytical results for the ion flow in the interaction region have been obtained [13,19] by approximating the ion guiding-center trajectories by straight lines. The important feature of the analysis is the truncation of the distribution function due to absorption of particles by the surface of the moon. Under this assumption the guiding-center distribution function for ions can be calculated everywhere.

In order to compute the perturbations of the interplanetary magnetic field, it is assumed that the total electric current induced in the perturbed lunar wake is composed of a) magnetization current, b) gradient drift current and c) curvature drift current[20].

In this treatment the lunar wake behind the moon is not cylindrically symmetrical but a plane of symmetry is defined by the direction of the interplanetary magnetic field and the solar wind velocity. The height of the lunar wake remains a constant two lunar radii transverse to this plane. In this plane the width varies depending upon field orientation and the temperature of the plasma. An important parameter is the speed ratio, S, defined by the ratio of the solar wind velocity, V_o, to the ion thermal speed parallel to the field lines, $V_{\parallel} = \sqrt{2kT_{\parallel}/m_i}$: $S = V_o/V_{\parallel}$.

The length of the wake varies depending upon the field orientation, ϕ, with the shortest wake obtained when the field lines are transverse to the solar wind flow. An infinitely long wake is predicted for a field line orientation parallel to the solar wind velocity with intermediate lengths obtained for oblique orientations.

The most critical parameter determining the magnitude of the field anomaly at a given speed ratio and orientation is β, which is a measure of the diamagnetic properties of the plasma given by the ratio of perpendicular plasma pressure, $P_{\perp} = nkT_{\perp}$, to magnetic field pressure, $B^2/8\pi$: $\beta = 8\pi nkT_{\perp}/B^2$.

Representative results of the kinetic theory are shown in Fig. 9 for a typical field orientation at the Archimedian spiral angle $\phi = 135^o$ and S=10, β = 1.0. Larger values of β lead to enhanced perturbations of the field magnitude and are consistent with experimental observations.

6.0 Summary

The experimental results from Explorer 35 have definitively established the nature of the lunar environment and the solar wind flow past the moon. The moon appears to be a nonmagnetic, relatively nonconducting and hence relatively cold dielectric sphere which absorbs both solar wind plasma and energetic particle fluxes which impact its surface[8,18].

The electrical conductivity structure and internal temperature of the moon may be very interesting additional results obtained from Explorer 35. As additional studies are conducted of the experimental data and an accurate theoretical model developed for the propagation past the moon of transient disturbances, such as MHD shocks and tangential discontinuities, more precise insight into the problem of the present state of the lunar interior will be gained.

7.0 Acknowledgements

I am pleased to acknowledge the participation of my colleagues K. W. Behannon, S. C. Cantarano, C. S. Scearce and Drs. H. E. Taylor and Y. C. Whang in the conduct of the NASA-GSFC magnetic field experiment.

7.0 References

1. Behannon, K. W., Intrinsic Magnetic Properties of the Lunar Body, NASA-GSFC preprint X616-68-171.

2. Colburn, D. S., R. G. Currie, J. D. Mihalov and C. P. Sonett, Diamagnetic Solar Wind Cavity Discovered Behind Moon, Science 158, 1040 (1967).

3. Dolginov, Sh. Sh., Ye. G. Yeroshenko, L. N. Zhuzgov, and I. A. Zhulin, Possible Interpretation of the Results of Measurements in the Near Lunar Satellite AMS Luna 10, Geomagnetizm i Aeronomiya, 7, 436 (1967). (In Russian).

4. England, A. W., Gene Simmons and D. Strangway, Electrical Conductivity of the Moon, J. Geophys. Res., 73, 3219 (1968).

5. Gold, T., The Magnetosphere of the Moon, in The Solar Wind, edited by R. J. Mackin, Jr., and N. Neugebauer, 381 Pergamon Press, New York (1966).

6. Hundhausen, A. J., S. J. Bame and N. F. Ness, Solar Wind Thermal Anisotropies: Vela 3 and IMP 3, J. Geophys. Res., 72, 5265 (1967).

7. Johnson, F. and J. E. Midgley, Note on the Lunar Magnetosphere, J. Geophys. Res., 73, 1523 (1968).

8. Lin, R. P., Observations of Lunar Shadowing of Energetic Particles, J. Geophys Res., 73, 3066 (1968).

9. Lyon, E. F., H. S. Bridge, J. H. Binsack, Explorer 35 Plasma Measurements in the Vicinity of the Moon, J. Geophys. Res., 72, 6113 (1967).

10. Ness, N. F., The Magnetohydrodynamic Wake of the Moon, J. Geophys. Res., 70, 517 (1965).

11. Ness, N. F., K. W. Behannon, C. S. Scearce, S. C. Cantarano, Early Results from the Magnetic Field Experiment on Lunar Explorer 35, J. Geophys. Res., 72, 5769, (1967).

12. Ness, N. F., K. W. Behannon, H. E. Taylor, Y. C. Whang, Perturbations of the Interplanetary Magnetic Field by the Lunar Wake, J. Geophys. Res., 73, 3421 (1968).

13. Serbu, P., Explorer 35 Measurements of Low Energy Plasma in Lunar Orbit, NASA-GSFC preprint X-615-68-232 (1968).

14. Siscoe, G. L., E. F. Lyon, J. H. Binsack and H. S. Bridge, An Interpretation of Explorer 35 Plasma Measurements in the Near Lunar Wake, MIT Center for Space Research Report CSR-TR-68-2, (1968).

15. Taylor, H. E., K. W. Behannon and N. F. Ness, Measurements of the Perturbed Interplanetary Magnetic Field in the Lunar Wake, J. Geophys. Res., 73, November (1968).

16. Tozer, D. C. and J. Wilson, The Electrical Conductivity of the Moon's Interior, Proc. Roy. Soc., A. 296, 320 (1967).

17. Tyler, G. L., Oblique-Scattering Radar Reflectivity of the Lunar Surface: Preliminary Results from Explorer 35, J. Geophys. Res., 73, to appear (1968).

18. Van Allen, J. A. and N. F. Ness, Particle Shadowing by the Moon, J. Geophys. Res., 73, to appear (1968).

19. Whang, Y. C., Interaction of the Magnetized Solar Wind with the Moon, Phys. Fluids, 11, 969, (1968).

20. Whang, Y. C., Theoretical Study of the Magnetic Field in the Lunar Wake, Phys. Fluids, 11, 1713 (1968).

SUMMARY OF LUNAR EXPLORER 35 RESULTS

Magnetic Moment	$M < 10^{20}$ cgs
Magnetic Susceptibility	$\mu_m < 1.8\ \mu_o$
Electrical Conductivity	$\sigma_m < 10^{-5}$ mhos/meter
Surface Dielectric Constant	$\varepsilon_s \approx 3\ \varepsilon_o$

No bow shock wave or lunar pseudo-magnetosphere. Absorption of solar wind by surface.

TABLE 1

FIGURE CAPTIONS

Figure 1 Gold and Tozer-Wilson theory of solar wind flow past moon.

Figure 2 Lunar Explorer 35 orbits July 1967-May 1968.

Figure 3 Measurements of near lunar magnetic field in October 1967 while in geomagnetic tail.

Figure 4 Measurements of near lunar magnetic field in April 1968 while in interplanetary space.

Figure 5 Simultaneous interplanetary magnetic field measurements by Explorers 33, 34 and 35 in September 1967. At this time, SEQ 73096 Explorer 35 is located at (-2.68, 0.34, 0.14) in SSE coordinates.

Figure 6 Diffusion-Convection time scales as function of bulk electrical conductivity of moon.

Figure 7 Electrical conductivity versus depth for various models of internal temperatures.

Figure 8 Reflectivity of lunar surface at 136 Megahertz and measurement of Brewster angle.

Figure 9 Results of Kinetic theory of solar wind flow past nonmagnetic nonconducting cold moon.

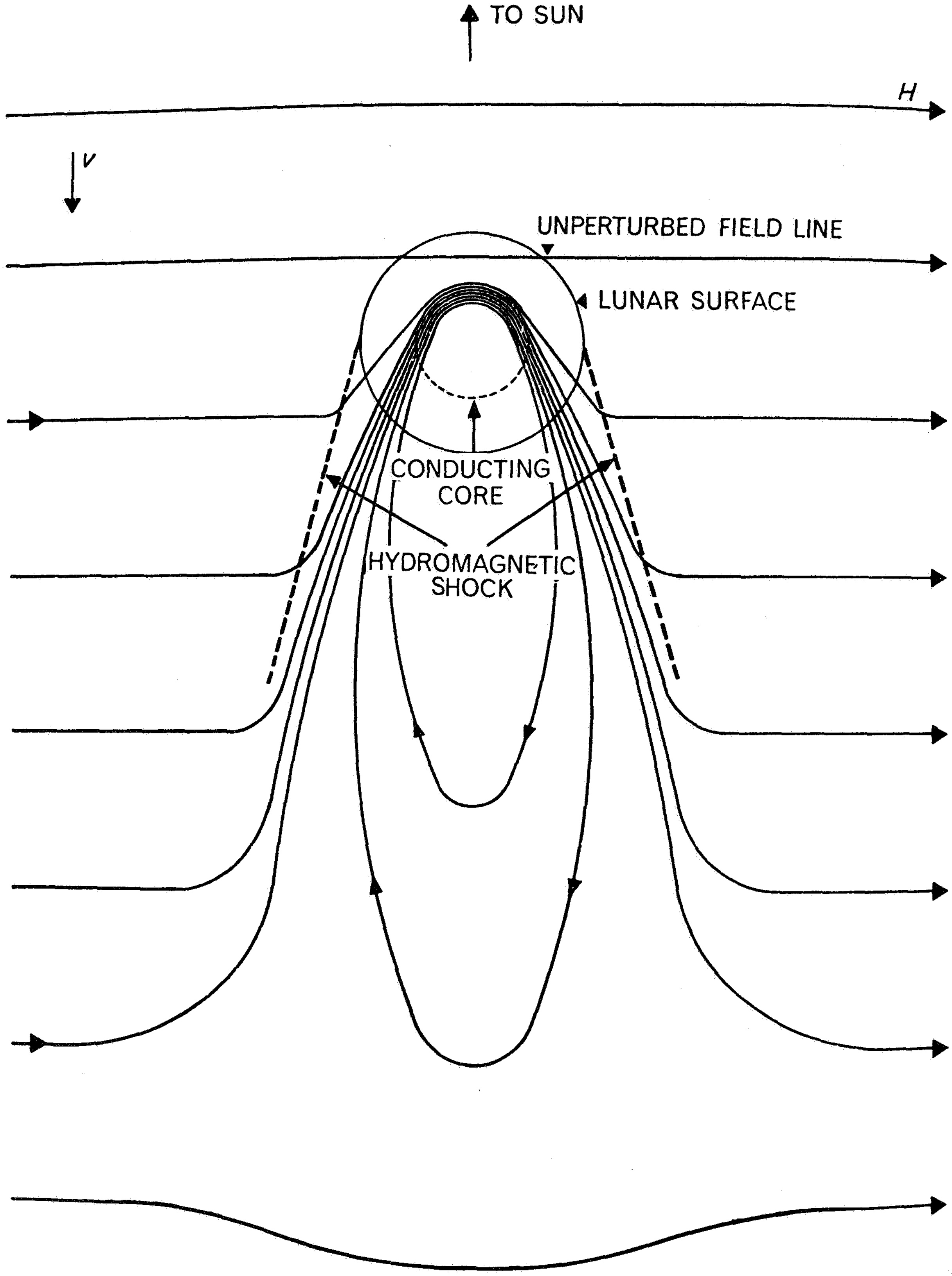
TO SUN
H
V
UNPERTURBED FIELD LINE
LUNAR SURFACE
CONDUCTING
CORE
HYDROMAGNETIC
SHOCK

FIGURE 1

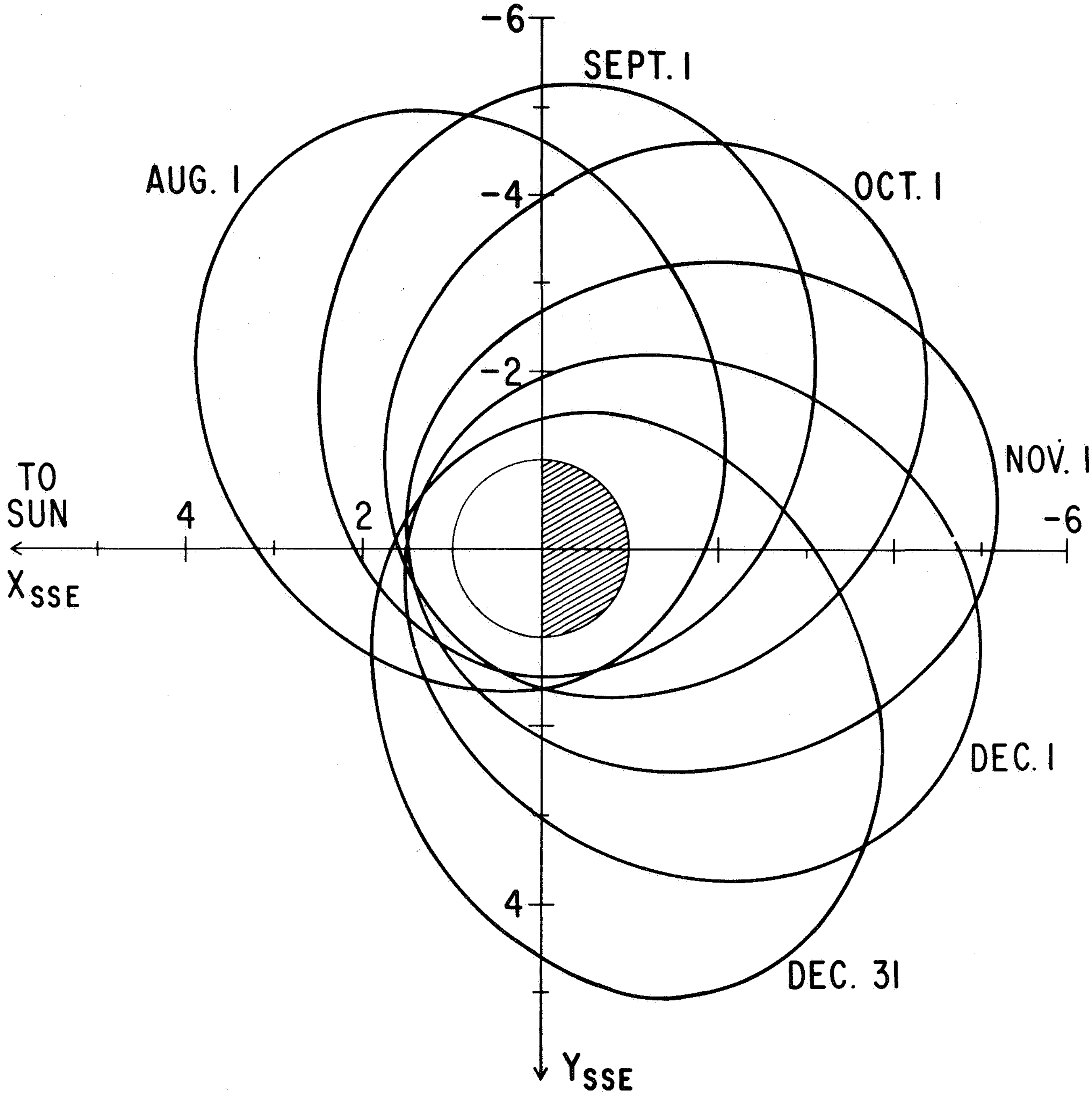

EXPLORER 35 ORBITS, 1967

FIGURE 2

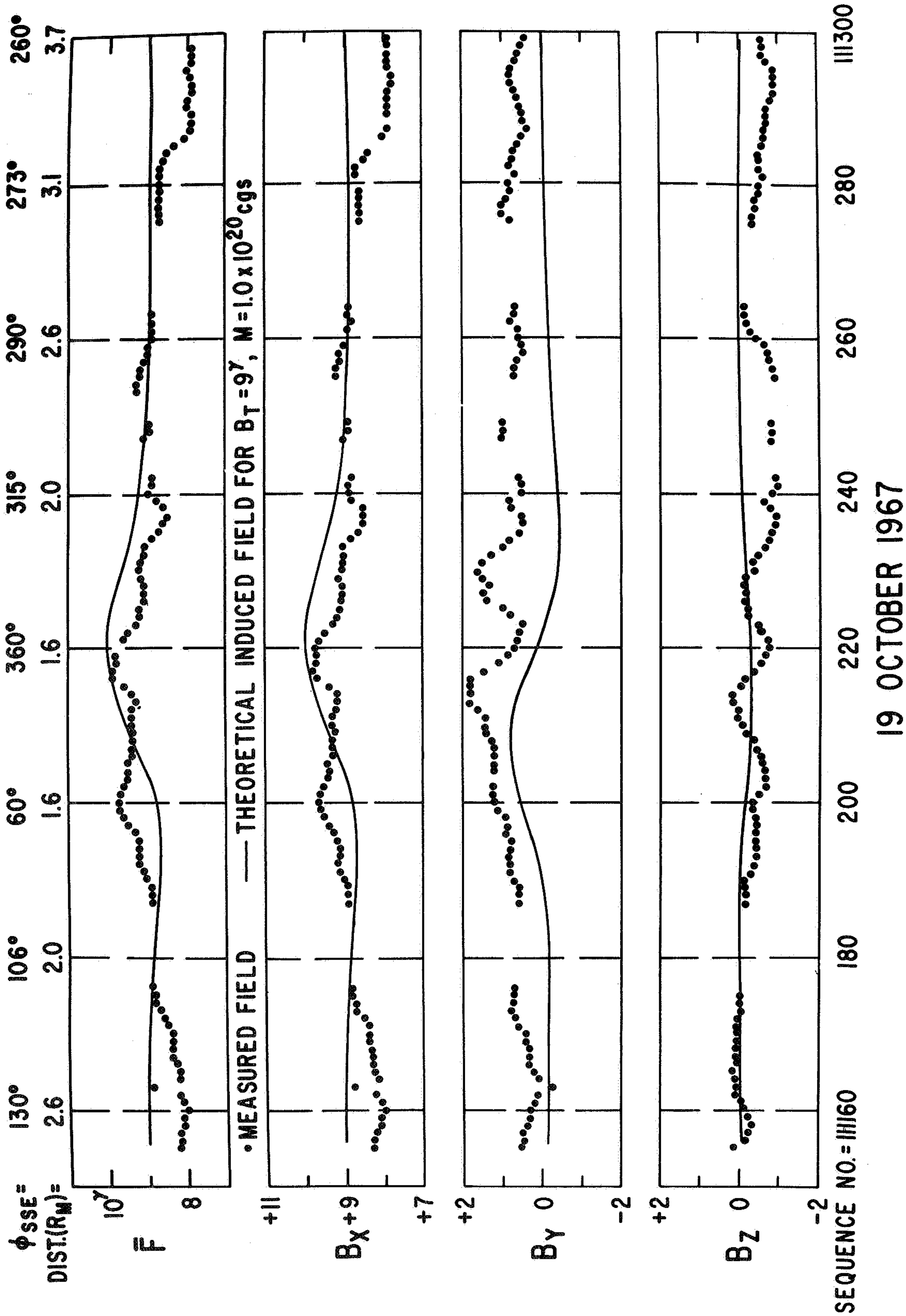

ϕSSE=
DIST.(RM)=
130° 2.6
106° 2.0
60° 1.6
360° 1.6
315° 2.0
290° 2.6
273° 3.1
260° 3.7
F
10γ
8
• MEASURED FIELD
— THEORETICAL INDUCED FIELD FOR BT=9γ, M=1.0x10^20 cgs
BX+9
+11
+9
+7
BY
+2
0
-2
BZ
+2
0
-2
SEQUENCE NO.=111160
180
200
220
240
260
280
111300
19 OCTOBER 1967

FIGURE 3

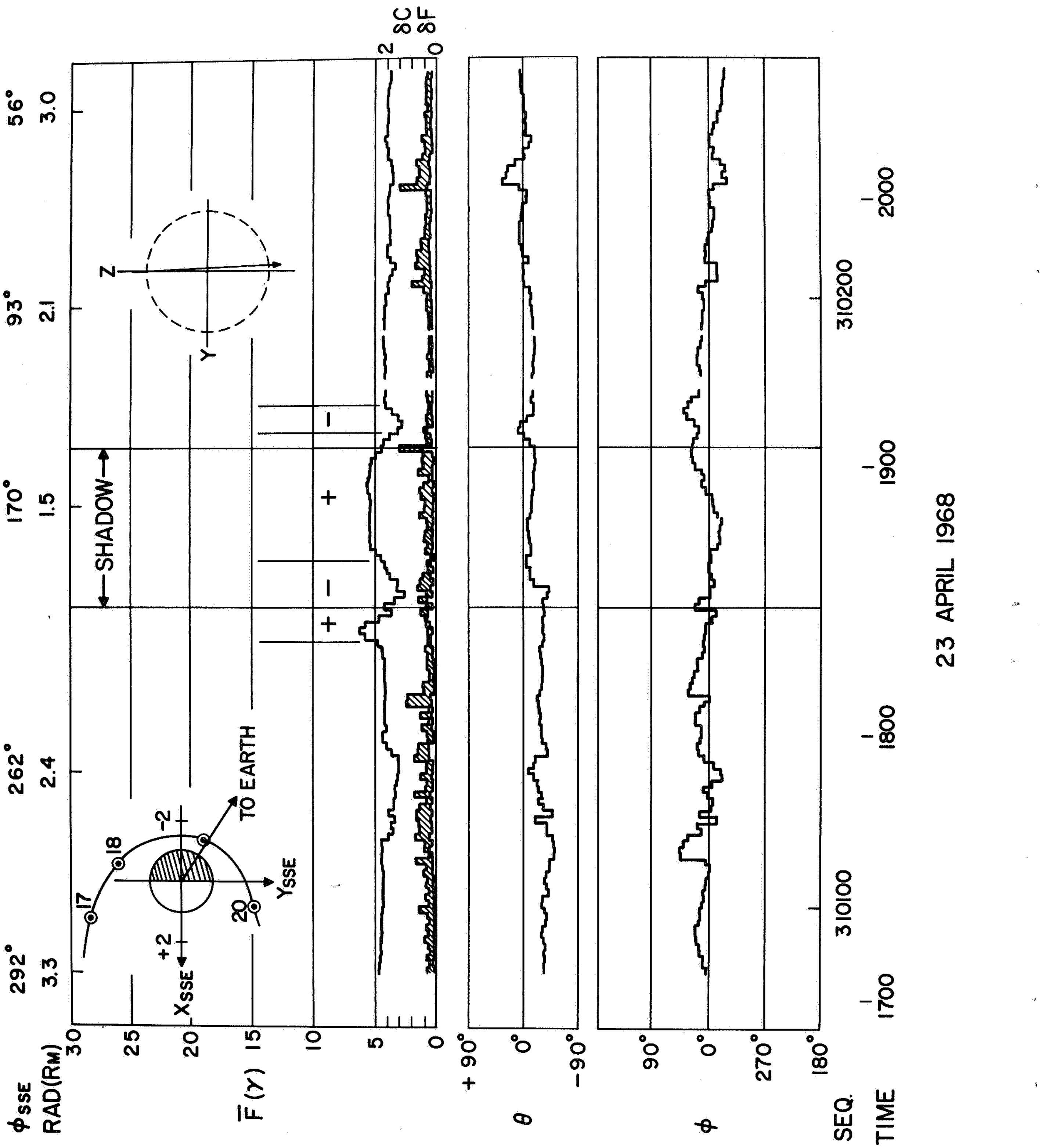

φSSE
RAD(RM)
F̄ (γ)
θ
φ
SEQ.
TIME
292°
262°
170°
93°
56°
3.3
2.4
1.5
2.1
3.0
30
25
20
15
10
5
0
+90°
0°
-90°
90°
0°
270°
180°
2
δC
δF
0
SHADOW
TO EARTH
XSSE
YSSE
+2
-2
17
18
20
Z
Y
+
-
310100
310200
1700
1800
1900
2000
23 APRIL 1968

FIGURE 4

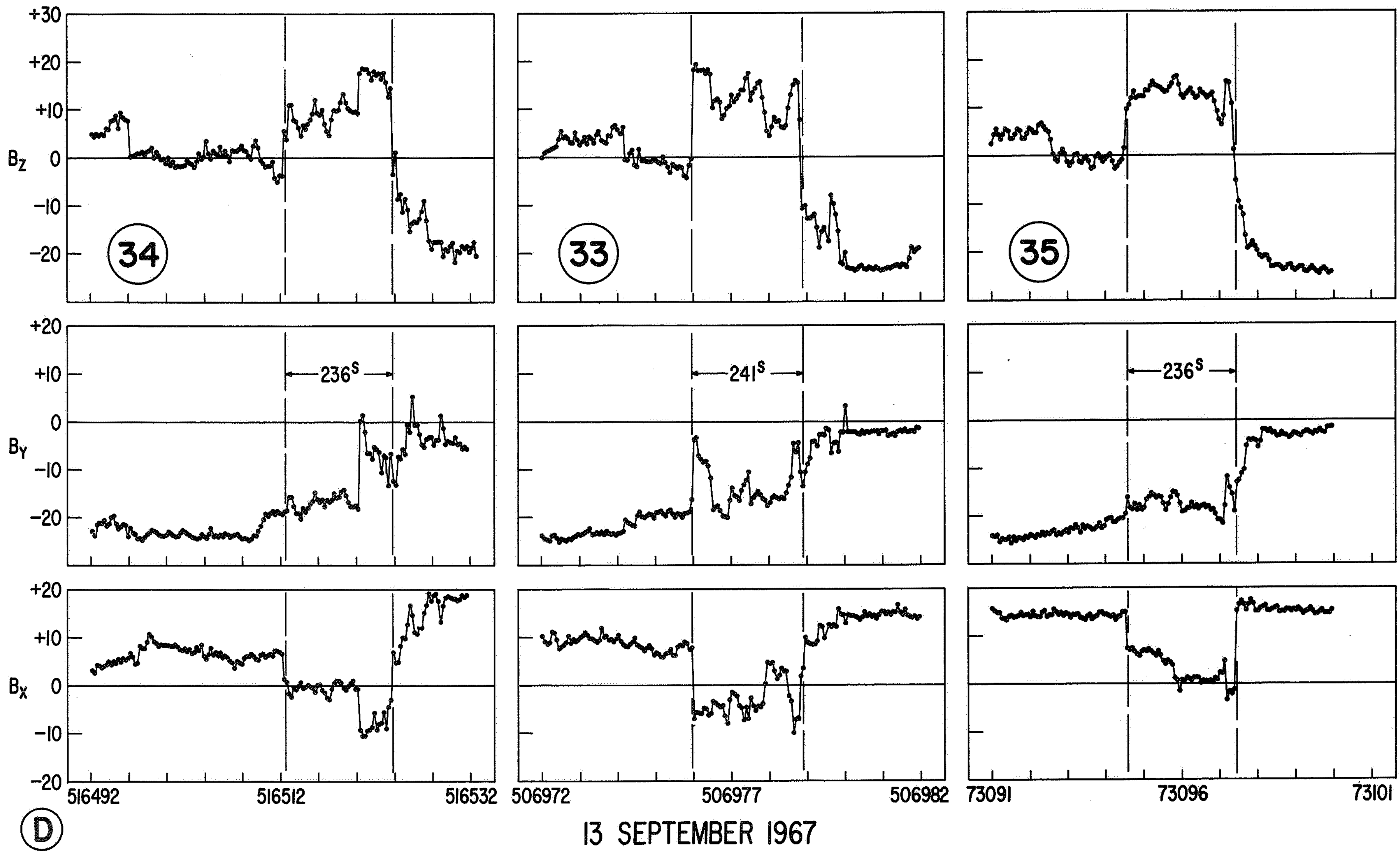

+30
+20
+10
0
-10
-20
B_Z
B_Y
B_X
34
33
35
236ˢ
241ˢ
236ˢ
516492
516512
516532
506972
506977
506982
73091
73096
73101
D
13 SEPTEMBER 1967

FIGURE 5

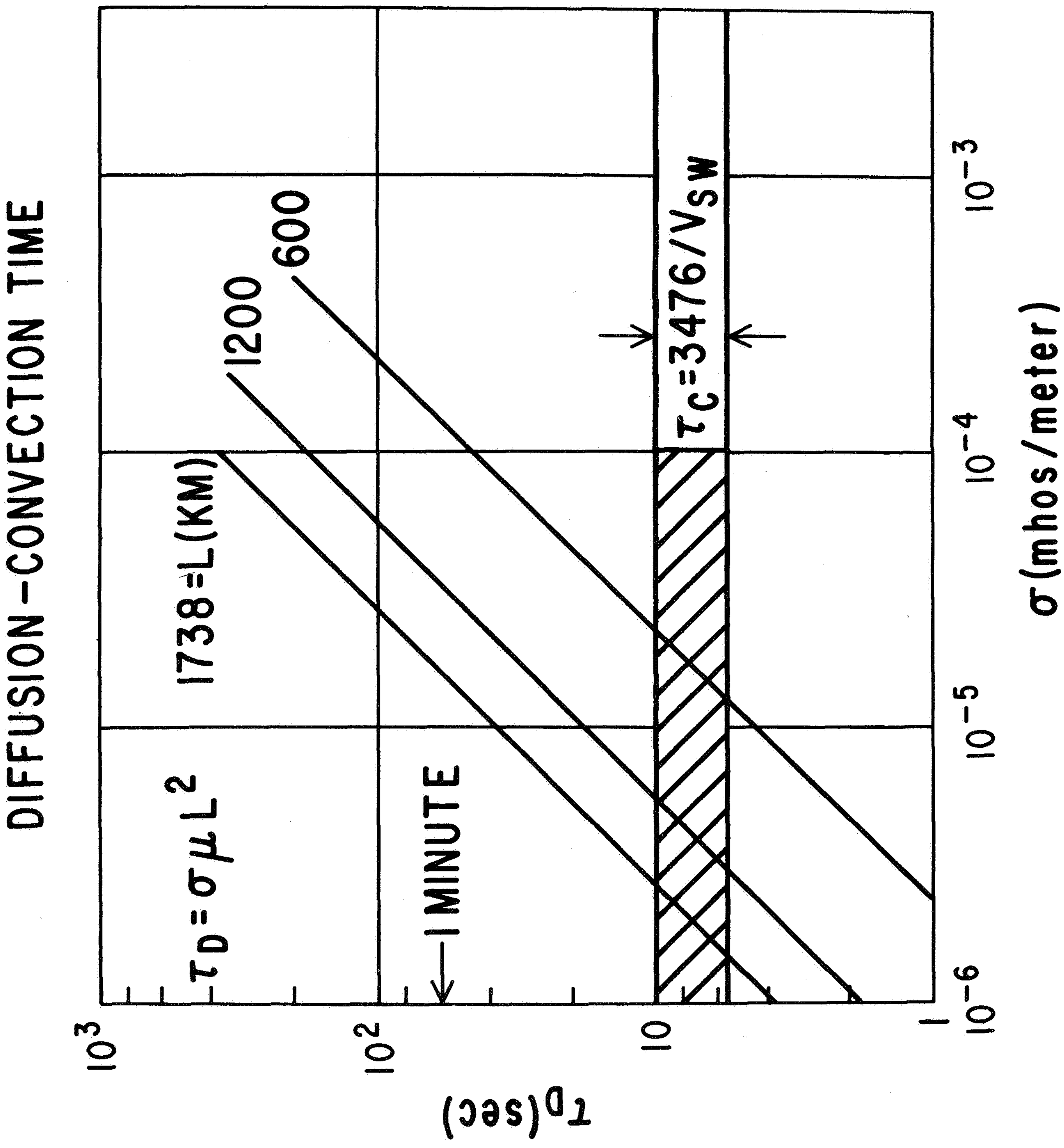
DIFFUSION-CONVECTION TIME
$\tau_D = \sigma \mu L^2$
1738=L(KM)
1200
600
$\tau_C = 3476/V_{SW}$
1 MINUTE
10^3
10^2
10
1
10^{-6}
10^{-5}
10^{-4}
10^{-3}
σ(mhos/meter)
τ_D(sec)

FIGURE 6

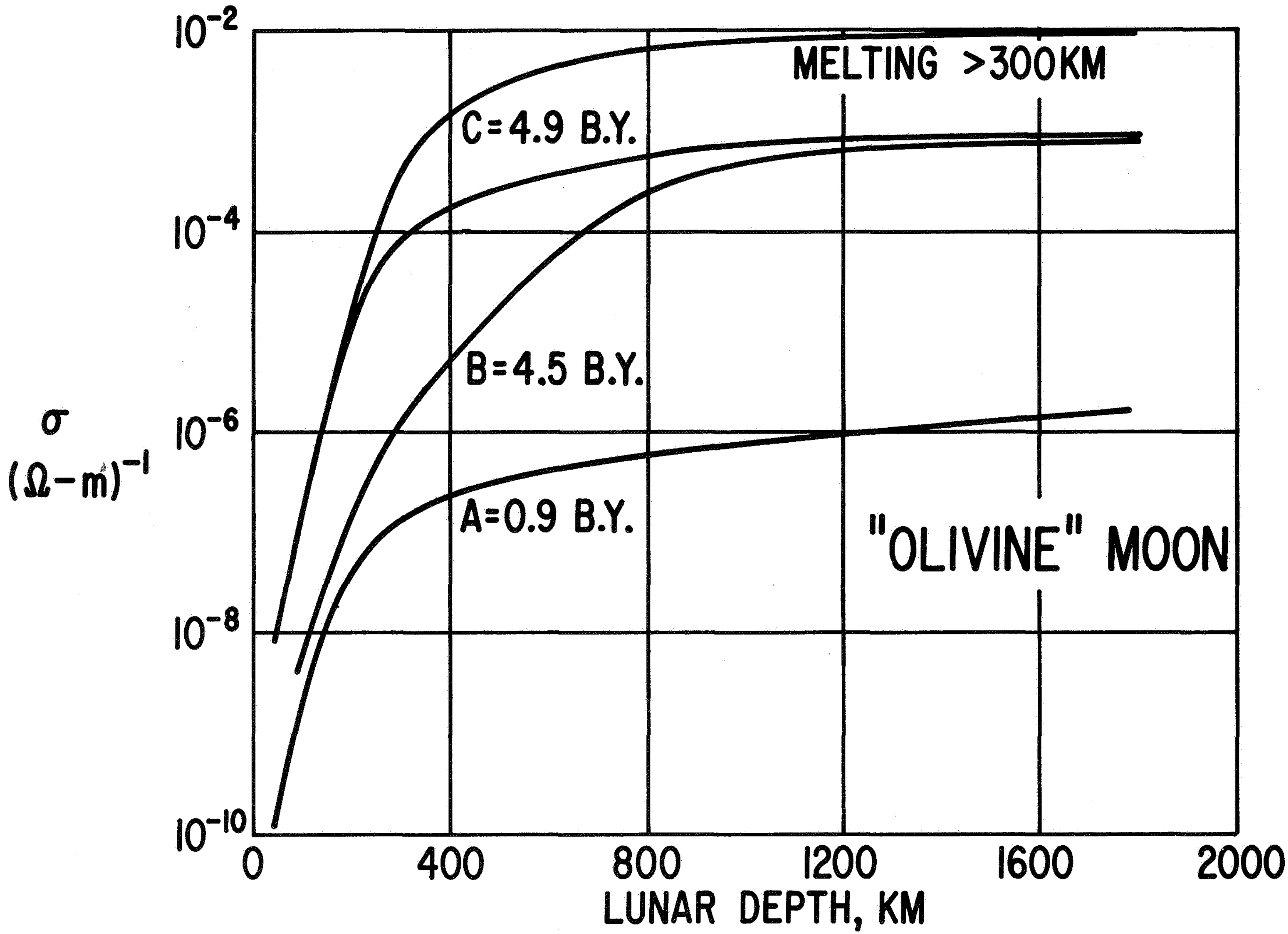
10^-2
10^-4
10^-6
10^-8
10^-10
σ (Ω-m)^-1
MELTING >300KM
C=4.9 B.Y.
B=4.5 B.Y.
A=0.9 B.Y.
"OLIVINE" MOON
0
400
800
1200
1600
2000
LUNAR DEPTH, KM

FIGURE 7

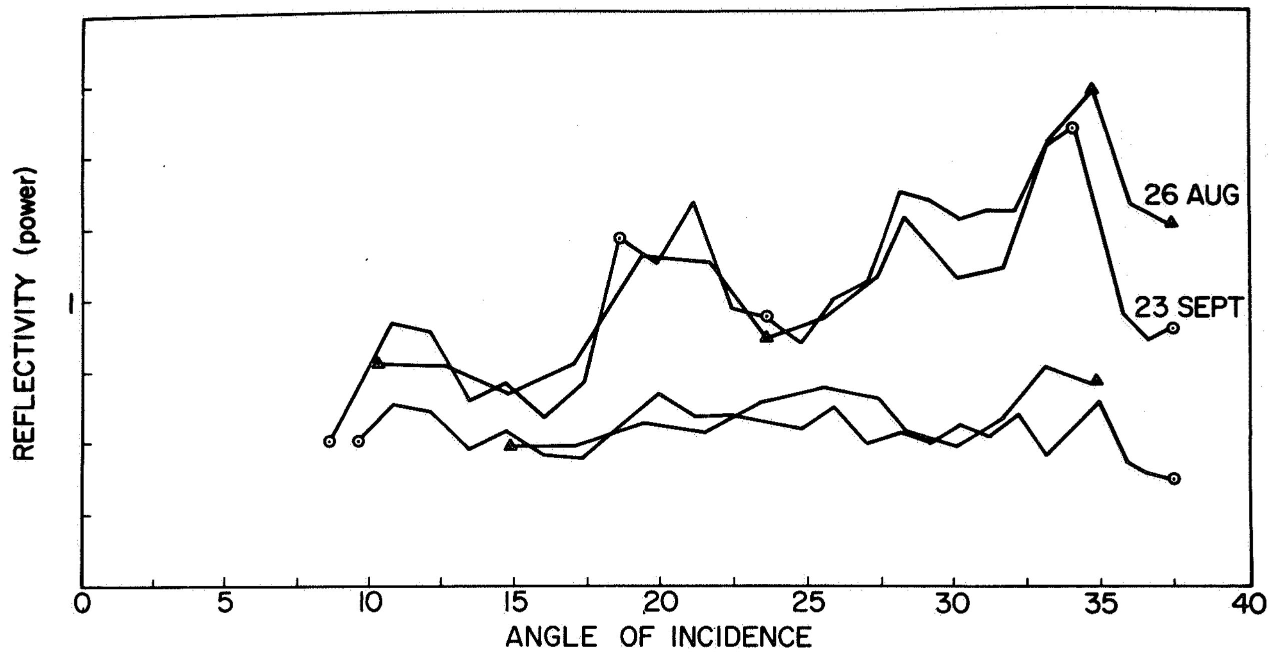

REFLECTIVITY (power)
1
26 AUG
23 SEPT
0
5
10
15
20
25
30
35
40
ANGLE OF INCIDENCE

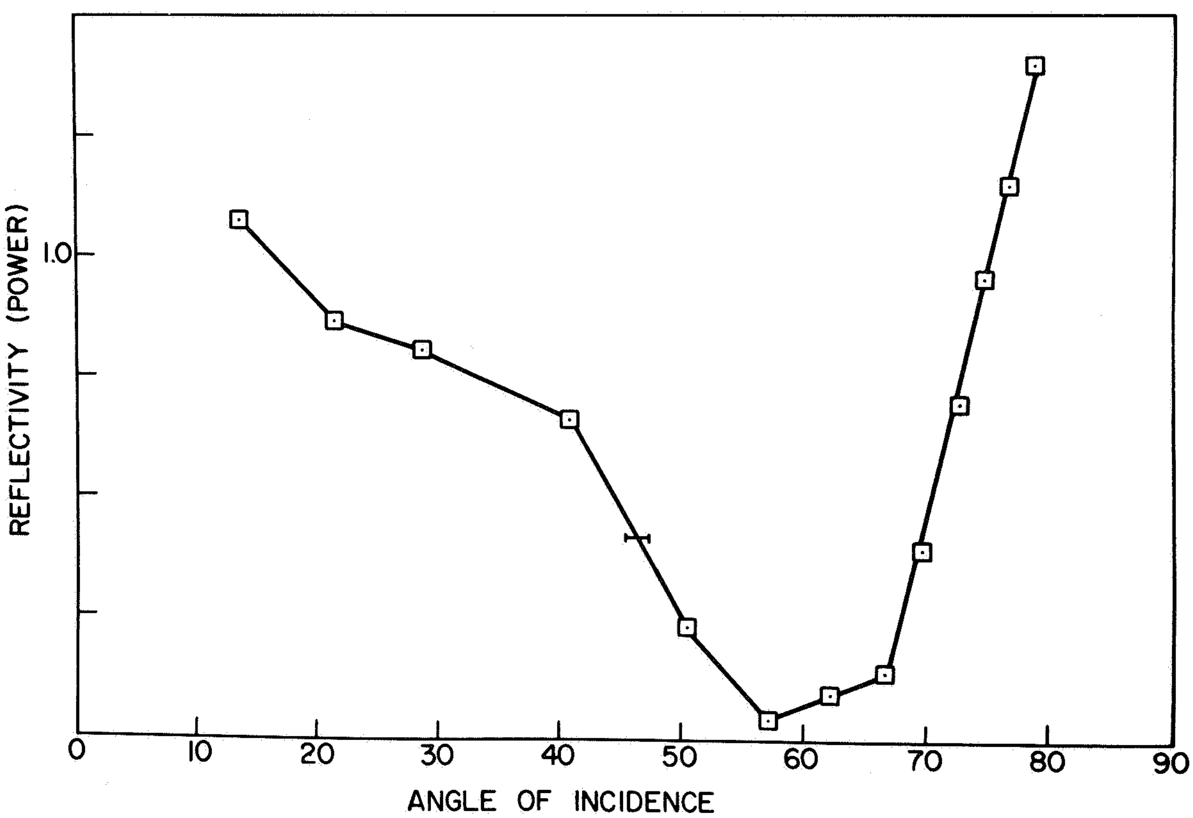

REFLECTIVITY (POWER)
1.0
0
10
20
30
40
50
60
70
80
90
ANGLE OF INCIDENCE

FIGURE 8

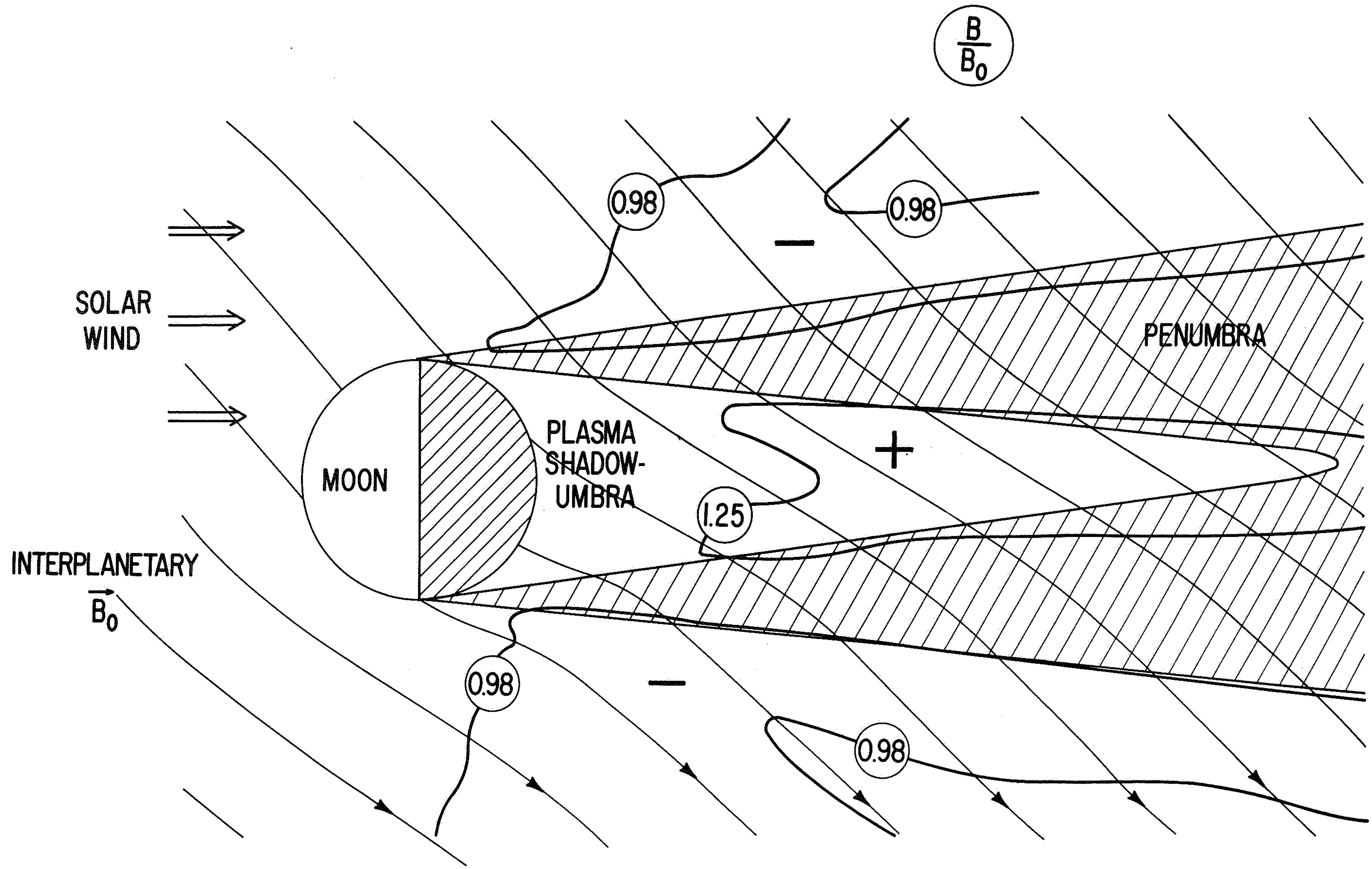
$\frac{B}{B_0}$
SOLAR WIND
INTERPLANETARY $\vec{B}_0$
MOON
PLASMA SHADOW-UMBRA
PENUMBRA
0.98
0.98
0.98
0.98
1.25
+
−
−

FIGURE 9